A Four Leg Shunt Active Power Filter Predictive Fuzzy Logic Controller for Low-Voltage Unbalanced-Load Distribution Networks

A. M. Fahmy[*], Ahmed K. Abdelslam[†], Ahmed A. Lotfy[**], Mostafa Hamad[**], and Abdelsamee Kotb[***]

[*]Department of Electrical Engineering, Canadian International College, Cairo, Egypt
[†,**]Department of Electrical and Control Engineering, Arab Academy for Science and Technology, Alexandria, Egypt
[***]Department of Electrical Engineering, Al-Azhar University, Cairo, Egypt

Abstract

Recently evolved power electronics' based domestic/residential appliances have begun to behave as single phase non-linear loads. Performing as voltage/current harmonic sources, those loads when connected to a three phase distribution network contaminate the line current with harmonics in addition to creating a neutral wire current increase. In this paper, an enhanced performance three phase four leg shunt active power filter (SAPF) controller is presented as a solution for this problem. The presented control strategy incorporates a hybrid predictive fuzzy-logic based technique. The predictive part is responsible for the SAPF compensating current generation while the DC-link voltage control is performed by a fuzzy logic technique. Simulations at various loading conditions are carried out to validate the effectiveness of the proposed technique. In addition, an experimental test rig is implemented for practical validation of the of the enhanced performance of the proposed technique.

Key words: 4-leg converter, 4-wire unbalanced distribution system, Fuzzy logic controller, Predictive controller, Shunt active power filter

I. Introduction

Modern sophisticated power electronic devices have led a worldwide evolution of high performance consumer electronics and appliances such as air conditions, washing machines, personal computers, etc. These devices perform as non-linear loads injecting voltage and current harmonics especially at the low voltage distribution level, which results in overheating of distribution transformers, malfunctioning of protection devices, and cross-talk interference with nearby equipment [1].

In addition to supplying current harmonics, unbalanced loads contributes to additive neutral current generation in four wire distribution networks, which may lead to double over-sizing the neutral wire in recently installed low-voltage grids [1], [2]. Hence, the need to mitigate fourth wire neutral current is a must in modern distribution power networks [1]-[3].

Four-wire shunt active power filters (SAPFs) can achieve several simultaneous tasks, among them neutral current mitigation, line current harmonic cancellation, and reactive power compensation.

Various SAPF topologies have been presented in the literature, where the 4-Leg, Split Capacitor and Cascaded H-Bridge are common examples [4]. Other dual function operations have been proposed for maximizing the benefits of an installed SAPF by adding extra functions such as renewable energy grid tied converter, UPS function, unified power quality control, etc. [5]-[9].

The core of SAPF operation is concerned with two main aspects: harmonic reference current generation and DC-link voltage control. For reference current generation, the classical p-q control is commonly utilized [10]-[15]. Hysteresis current control can be adopted based on either p-q theory or load current detection, yet it suffers from variable switching losses [16]-[18].

For a more precise harmonic current extraction, adaptive filters can be utilized in SAPF current extraction, but the performance is highly dependent on designer experience and

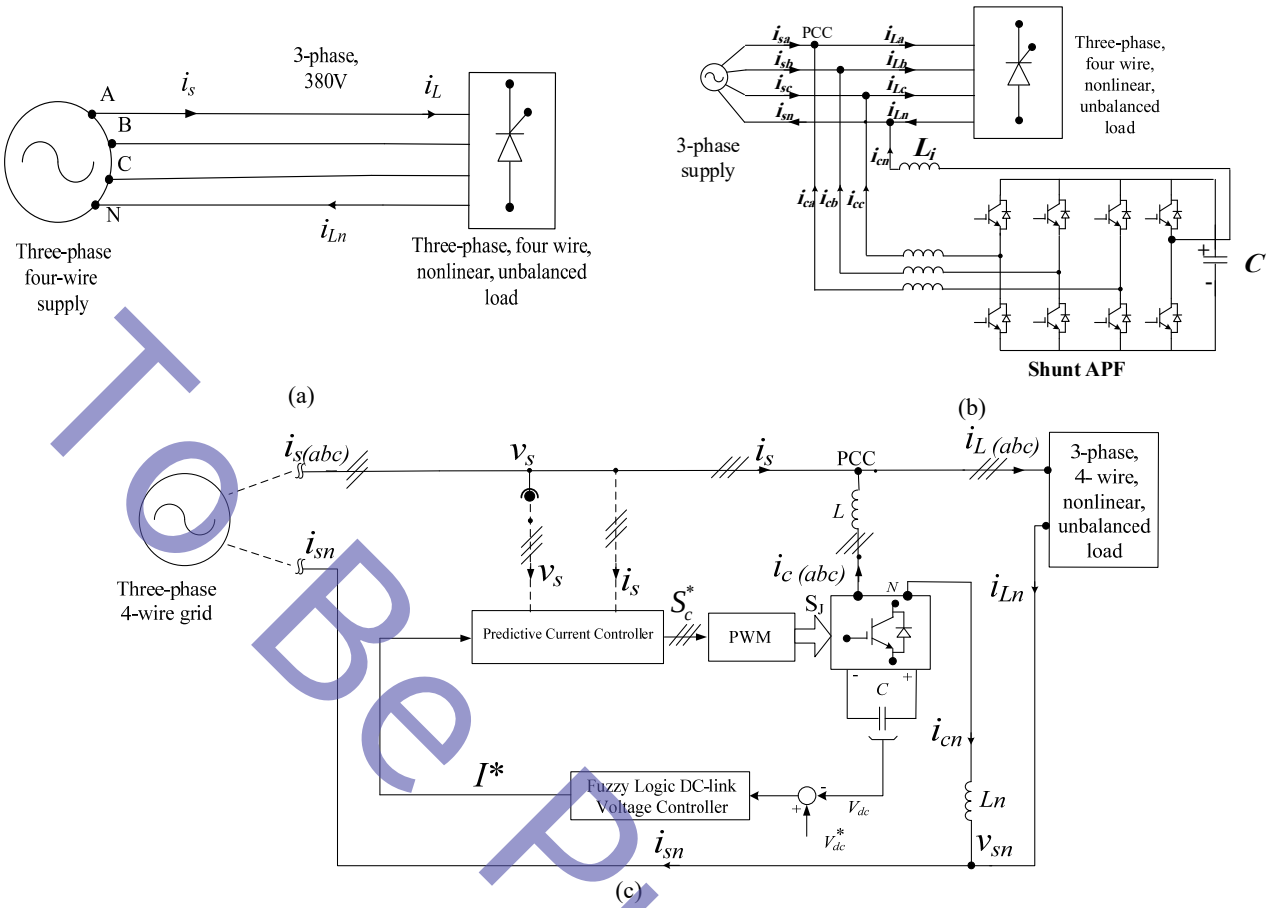

Fig. 1. Low-voltage distribution network under investigation. (a) Three-phase four-wire supply feeding a three-phase four-wire unbalanced non-linear load. (b) 4-Leg SAPF connected to the system under investigation. (c) Proposed SAPF controller block diagram.

complex algorithms for the filter design to compensate for a measured signals delay [19]-[22]. The one-cycle-control algorithm can be considered as a powerful tool for harmonic current extraction in a SAPF since it does not require a phase-locked loop or utility voltages.

The main drawback of this technique is the need of a systematic method for global dynamic analysis and a design tool specially when the input signal of the converter switch is a function of the output signal of that switch as in the case of SAPF converters [23]-[27]. Artificial neural networks (ANNs) can be utilized as harmonic current extractors for a SAPF. However, they require massive off-line training sets which is a major limitation [28]-[31]. The evolution of predictive control with its several advantages enables its utilization as a powerful tool for SAPF harmonic current extractors [32], [33]. The use of predictive controllers in a SAPF incorporates several advantages since no PLL is required, no previous training/designer based tuning is needed, and the load currents do not need to be measured [32], [34]-[36].

In terms of the DC-link voltage control, conventional Ziegler-Nichols tuned Proportional-Integral (PI) controllers suffers from a trade-off between a sluggish response and a transient over-shoot [37], [38]. The recently developed inverse control technique offers improved DC-link voltage dynamics when actual detailed period average dynamic system modeling is developed, which suffers from the common system elements' aging effect that deteriorates system performance [39, 40]. Fuzzy logic controllers offer enhanced system performance, better dynamic and steady-state response yet still need designer experience in determining the required fuzzification rules and membership functions [41]-[44].

In this paper, a predictive-fuzzy logic hybrid SAPF controller is proposed. The presented technique does not require a PLL. In addition, only the supply current, supply voltage and DC-link voltage need to be measured. The proposed algorithm shows enhanced DC-link voltage performance at start-up, transient and steady-state conditions. The predictive current control succeeds in attaining balanced supply currents and mitigated neutral currents. In addition, it achieves a near-unity power factor with a fast dynamic response under varying loading conditions.

This paper is organized into six sections. Following the introduction, the second section illustrates the system under investigation. The proposed hybrid predictive fuzzy logic based control is explained in the third section. System performance investigations of the proposed algorithm using simulation results is discussed in the fourth section. For more clarification of the proposed algorithm effectiveness, an experimental setup

and practical results at the transient and steady-state conditions are shown in the fifth section. Finally some conclusions are given in the sixth section.

II. System under Investigation

The investigated low-voltage distribution network incorporates a three-phase four-wire supply that feeds a three-phase four-wire non-linear unbalanced load. A system block diagram is shown in Fig. 1(a). This system suffers from supply current harmonics, supply current unbalance, and an undesirable neutral wire current. To sort out these power quality issues, a four-wire SAPF is connected at the Point of Common Coupling (PCC) between the supply and the load terminals with the 4-leg topology shown in Fig. 1(b).

III. Proposed 4-leg SAPF Hybrid Predictive Fuzzy Logic Controller

A 4-leg shunt APF is connected at the PCC to a three-phase four-wire grid through interfacing inductors for load current harmonics compensation, power factor improvement and supply currents balancing. The neutral wire is tied to the fourth leg in order to effectively mitigate the neutral current.

The proposed 4-leg APF control system block diagram is shown in Fig. 1(c). The presented controller requires measurement of the supply voltage and supply current at the PCC, in addition to the DC-link voltage of the APF. Measurements of the load current and injected filter current are not required. The APF reference current is extracted using DC-link capacitor voltage control. The DC-link capacitor voltage V_{dc} is subtracted from the reference voltage, V^*_{dc}. A DC-Link voltage controller acts on the resultant error. The DC-link voltage is kept constant and the power balance between the supply, the SAPF, and the load is achieved since the capacitor instantaneously compensates the difference between the supply and the load power. Multiplication of the DC-Link voltage controller output by the PCC per unit voltage forms the supply current reference. No supply voltage harmonics are considered.

A. Proposed Predictive Current Controller

The relation between SAPF current, i_c, the inverter output voltage, v_c, and the grid voltage at the PCC, v_s, is defined in discrete form by:

$$v_c^*(k+1) = \frac{L_i}{T_s}\left(i_c^*(k+1) - i_c(k)\right) + v_s(k) \quad (1)$$

where L_i is the interfacing inductance, T_s is the sampling time, and $i_c^*(k+1)$ and $v_c^*(k+1)$ are the predicted reference current and the predicted reference output voltage of the SAPF at the sampling instant $(k+1)$, respectively.

The SAPF current i_c at the sampling instant k is:

$$i_c(k) = i_L(k) - i_S(k) \quad (2)$$

where i_L is the load current, and i_s is the grid current at the sampling instant k. Since the sampling instant $(k + 1)$ is not available, $i_c^*(k+1)$ is assumed to be equal to $i_c^*(k)$. This introduces a one sample time delay which is less significant if the sampling frequency is high [1], [2].

The SAPF reference i_c^* current can be expressed as:

$$i_c^*(k) = i_L(k) - i_S^*(k) \quad (3)$$

Hence, the predicted SAPF output voltage can be expressed in terms of the reference and actual grid currents by:

$$v_c^*(k+1) = \frac{L_i}{T_s}\left(i_s(k) - i_s^*(k)\right) + v_s(k) \quad (4)$$

In addition to compensating the supply current harmonics, the SAPF is controlled to achieve a balance of the three-phase currents. The load neutral current is given by:

$$i_{Ln}(k) = i_{La}(k) + i_{Lb}(k) + i_{Lc}(k) \quad (5)$$

Similarly, the SAPF output for the forth-leg can be represented by:

$$v_{cn}^*(k+1) = \frac{L_i}{T_s}\left(i_{cn}^*(k+1) - i_c(k)\right) + v_{sn}(k) \quad (6)$$

$$i_{cn}(k+1) = i_{sn}(k+1) - i_{Ln}(k) \quad (7)$$

$$i_{cn}^*(k+1) = i_{sn}^*(k+1) - i_{Ln}(k) \quad (8)$$

where i_{sn}, i_{sn}^*, i_{cn}, i_{cn}^*, i_{Ln} and v_{sn} are the grid neutral current, reference grid neutral current, SAPF neutral current, reference SAPF neutral current, load neutral current and grid voltage at the neutral point, respectively. Hence:

$$v_{cn}^*(k+1) = \frac{L_i}{T_s}\left(i_{sn}^*(k+1) - i_{sn}(k)\right) + v_{sn}(k) \quad (9)$$

However:

$$i_{sn}^*(k+1) = 0 \quad (10)$$

$$v_{sn}(k) = 0 \quad (11)$$

$$i_{sn}(k) = i_{sa}(k) + i_{sb}(k) + i_{sc}(k) \quad (12)$$

Then:

$$v_{cn}^*(k+1) = -\frac{L_i}{T_s} i_{sn}(k) = -\frac{L_i}{T_s}\left(i_{sa}(k) + i_{sb}(k) + i_{sc}(k)\right) \quad (13)$$

The above equations are used to predict the modulating signals necessary to generate the SAPF pulse width modulation (PWM) for both the three-phase and the forth-leg. Hence, the supply current and voltage becomes in phase and the grid supplies only active power to the load. The predictive control method proposed for the 4-leg SAPF can compensate both the grid current harmonics and the unbalance. Thus, it mitigates the neutral current and improves the power factor. It offers a simple realization, a reduced number of sensors and no PLL is required.

B. Proposed DC-Link Voltage Fuzzy Logic Controller

A Mamdani's type fuzzy logic controller [43], [44] is proposed for the SAPF DC-link voltage control.

The actual DC-link voltage V_{dc} is compared to the reference value V_{dc}^*. The error (E) can be expressed as:

$$E = V_{dc}^* - V_{dc} \quad (14)$$

The error (E) and change of error (CE) signals are processed through a fuzzy controller, as shown in Fig. 2(a), which contributes to the near zero steady-state error in tracking the reference current. In addition, the controller

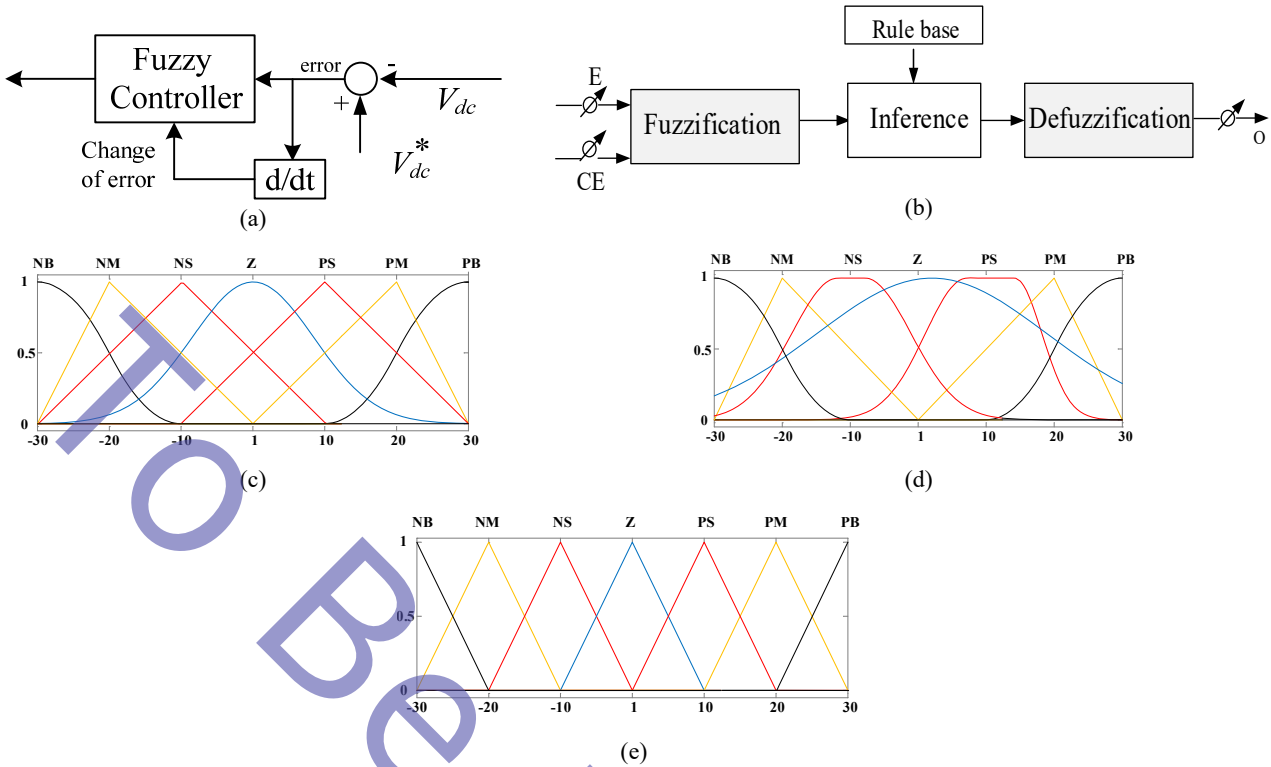

Fig. 2. Proposed DC-link voltage fuzzy logic controller. (a) Controller block diagram. (b) FLC stages. (c) Error membership function. (d) Change of error membership function. (e) Output membership function.

TABLE I
FUZZY RULES BASE

E / *CE*	NB	NM	NS	Z	PS	PM	PB
NB	PB	PB	PM	PB	PS	PS	Z
NM	PB	PB	PM	PM	PS	Z	NS
NS	PM	PM	PM	PS	Z	NS	NM
Z	PM	PS	PS	Z	NS	NM	NM
PS	PS	PS	Z	NS	NS	NM	ZM
PM	PS	Z	NS	NM	NM	NM	NB
PB	Z	NS	NS	NM	NM	NB	NB

limits the overshoot and inrush current during the transient state.

The fuzzy logic controller is independent of the system model. The design is mainly based on intuitive feeling and designer experience. The rules are expressed as follows: (the error *E* is X; and the change of error *CE* is Y) then (the control output is O).

For enhanced performance of the controller, the fuzzy petitioned subspaces negative big (NB), negative medium (NM), negative small (NS), zero (Z), positive small (PS), positive medium (PM), and positive big (PB) are used. These seven membership functions are similar for the inputs and output. The FLC rules are summarized in Table I.

The main parts of the proposed FLC including the fuzzification, rule-base, inference and defuzzification, are shown in Fig. 2(b). The membership functions (MFs) for the error, change of error and output variables are shown in Fig. 2 parts (c), (d) and (e), respectively.

The selection and tuning of the MFs is performed using the MATLAB® Fuzzy Logic Toolbox, see the Appendix for design steps illustration of the MFs.

IV. SIMULATION RESULTS

A 4-leg SAPF is connected at the PCC to a three-phase four-wire grid through interfacing inductances with a neutral wire tied to the fourth leg. The system under investigation, shown in Fig. 1(c), is simulated using MATLAB/Simulink® to investigate its performance. The PCC voltage is 380 V. The non-linear load is represented by a three-phase diode rectifier feeding an inductive load consists of a resistor R_{L1}= 30 Ω and an inductor L_{L1}=150 mH acting as a harmonic current source. The current unbalance is presented by connecting an inductive load with phase A consisting only of a resistor R_{LN}= 15 Ω and an inductor L_{LN}=50 mH. The resistance and the inductance of the SAPF coupling inductor, are R_i = 0.01 Ω and L_i = 4 mH, respectively. A DC-link capacitor of 3 mF is used.

The reference DC-link voltage is set to 650V, and the inverter switching frequency, f_s, is 5 kHz.

The SAPF is switched on at 0.04s and the load is increased at 0.2s by connecting the inductive load of the resistor R_{L2}= 50 Ω and the inductor L_{L2}=50 mH in parallel to the existing three phase load. The DC-link voltage under the proposed fuzzy logic controller is shown in fig 3 (a). The SAPF starts

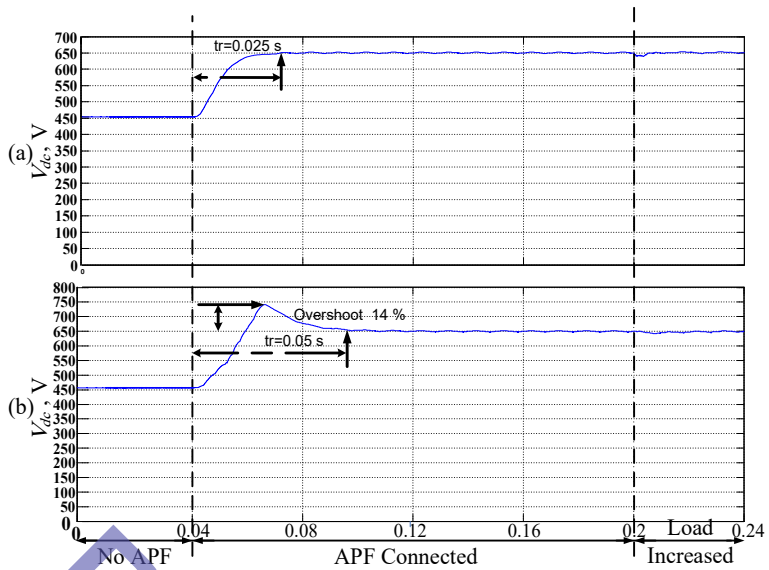

Fig. 3. DC-link capacitor voltage simulation results under: (a) proposed fuzzy logic controller; (b) conventional PI controller.

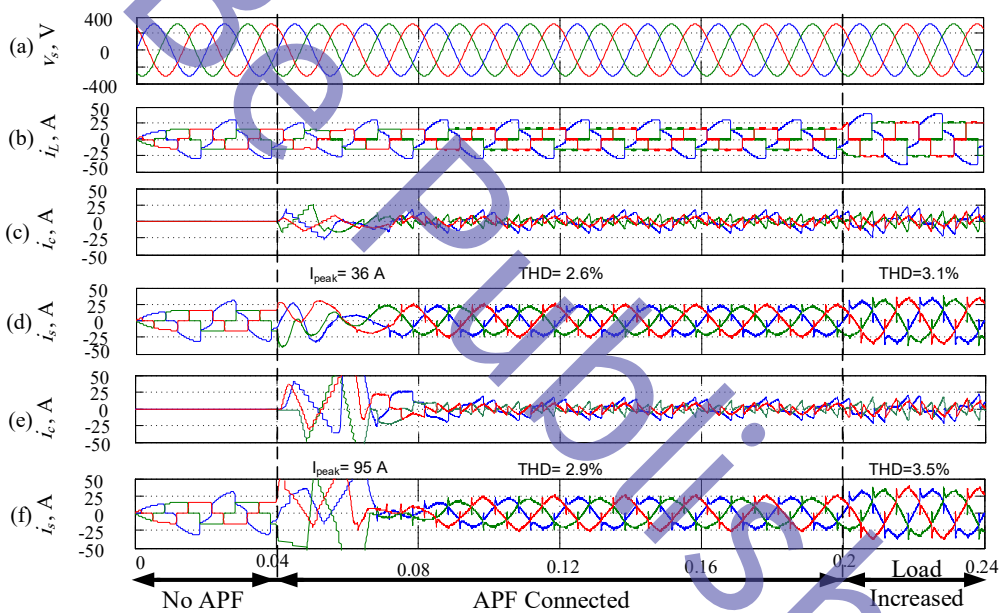

Fig. 4. System simulation results. (a) Supply voltage, v_s. (b) Load current, i_L. (c) SAPF current with a predictive fuzzy controller, i_c. (d) Supply current with a predictive fuzzy controller, i_s. (e) SAPF current with a predictive PI controller, i_c. (f) Supply current with a predictive PI controller, i_s.

at 0.04s while the DC-link voltage builds up fast to its reference of 650V at 0.065s, with no overshoot when compared with Fig. 3(b). This demonstrates the DC-link voltage performance under the conventional PI controller, where the voltage suffers an overshoot to 740V and stabilize to its reference of 650V at 0.09s. The three-phase grid voltage waveform at the PCC is shown in Fig. 4 (a).

A typical non-linear load current, i_L, is shown in Fig. 4(b). It is shown that the load current is distorted and unbalanced because of the bridge rectifier loading effect and the parallel unbalanced load. The APF current, i_c, shown in Fig. 4(c), with the proposed predictive fuzzy controller is injected at the PCC. As a result, a sinusoidal and balanced grid current, i_s, is achieved as illustrated in Fig. 4(d). A similar simulation was carried out for the system under investigation but with the conventional PI controller for the DC-link voltage control loop instead of the proposed fuzzy logic one. Simulation results are represented in Fig. 4 parts (e)-(f) for the SAPF current i_c and the grid current i_s, respectively. It can be easily observed from Fig. 4 parts (d) and (f) that the proposed predictive fuzzy logic controller achieves a better THD and less overshoot for the grid current when compared to the conventional PI controller when utilized as the SAPF DC-link voltage controller.

Under the proposed predictive fuzzy logic control algorithm, the grid neutral current i_{sn} is mitigated, as shown in

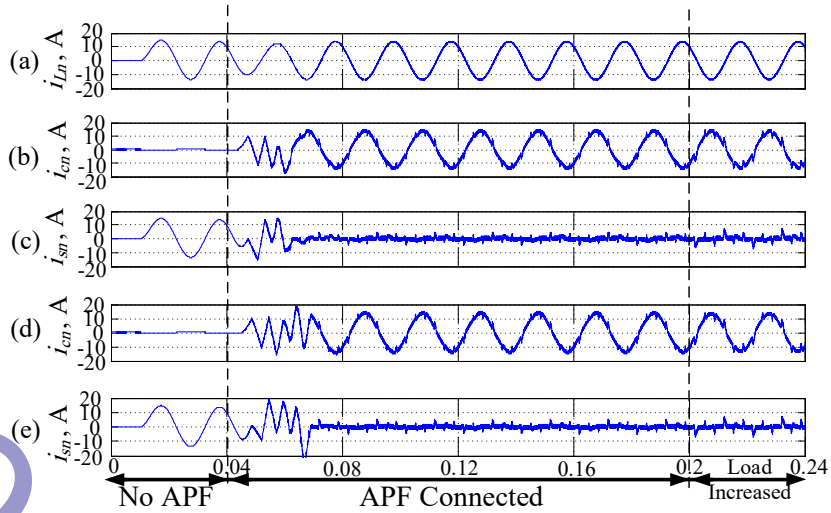

Fig. 5. System simulation results. (a) Load neutral current, i_{Ln}. (b) SAPF neutral current with a predictive fuzzy controller, $i_{\not\exists}$. (c) supply neutral current with a predictive fuzzy controller, i_{sn}. (d) SAPF neutral current with a predictive PI controller, i_{cn}. (e) Supply neutral current with a predictive PI controller, i_{sn}.

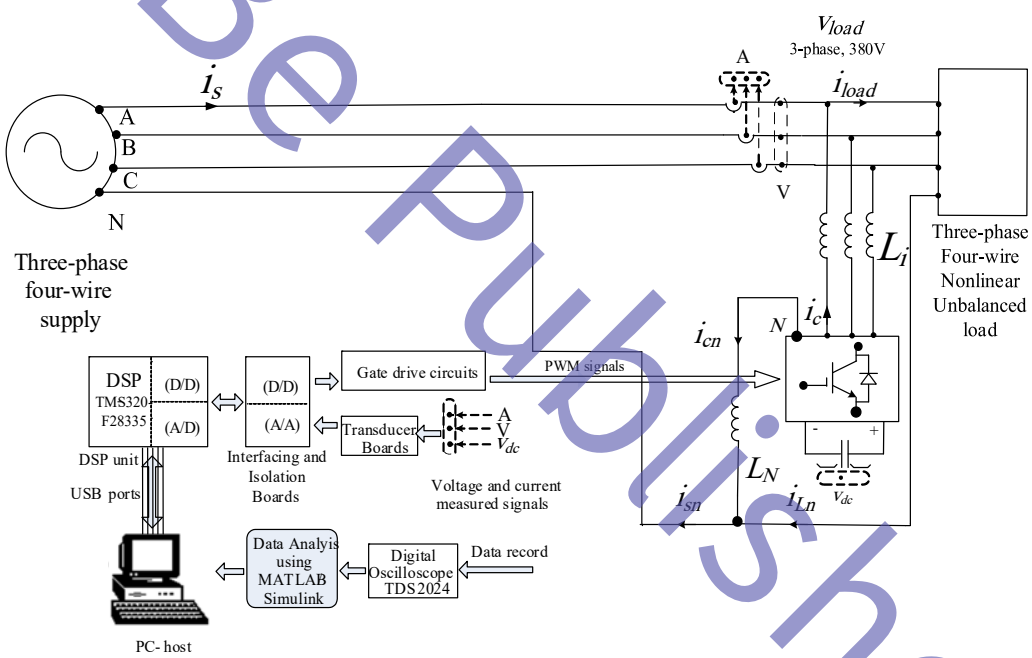

(a)

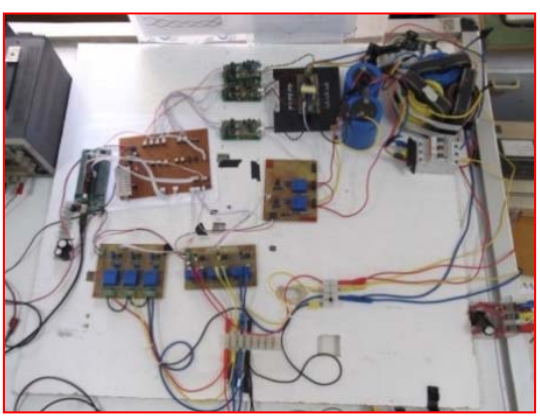

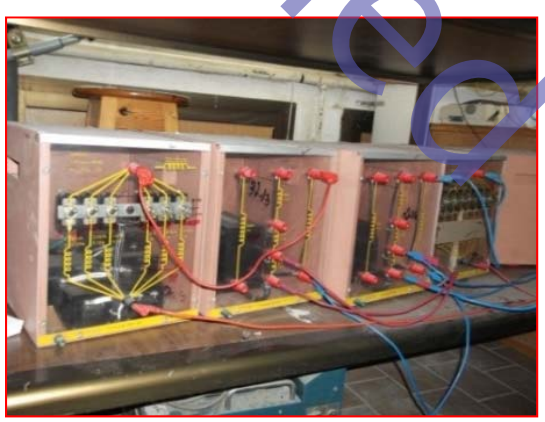

(b) (c)

Fig. 6. Experimental setup. (a) Experimental system block diagram. (b) Photograph of the test rig. (c) Three phase unbalanced load.

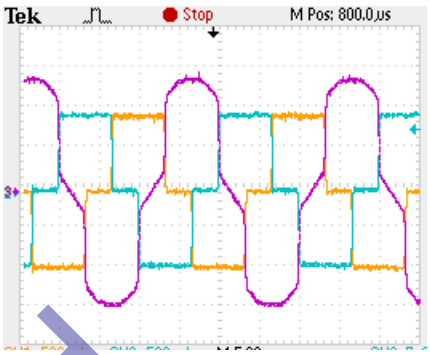

5 ms/div, ch1: 10 A/div, ch2: 10 A/div, ch3: 10 A/div

(a)

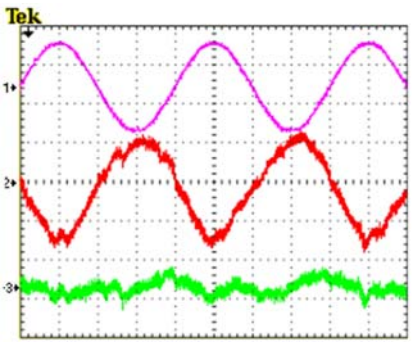

10 ms/div, ch1: 200 V/div, ch2: 200 V/div

(b)

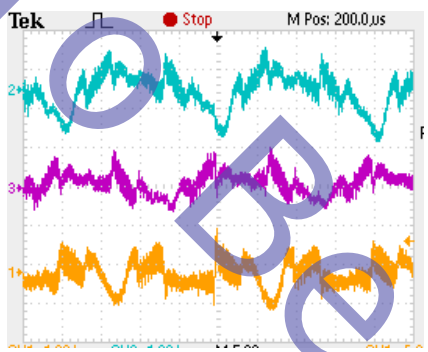

5 ms/div, ch1: 10 A/div, ch2: 10 A/div, ch3: 10 A/div

(c)

(d)

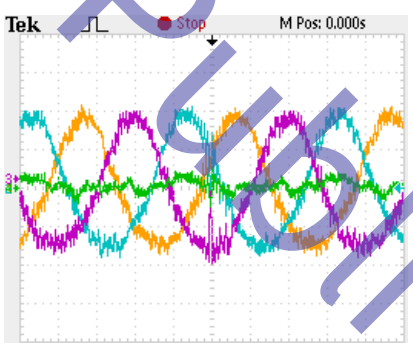

ms/div, ch1: 10 A/div, ch2: 10 A/div, ch3: 10 A/div, ch4: 10 A/div

(e)

Fig. 7. System experimental results. (a) Distorted unbalanced load current, $i_{L.}$ (b) DC-link voltage. (c) SAPF compensating currents, $i_{cabc.}$ (d) Load neutral current, i_{Ln}, SAPF neutral compensating current, i_{cn}, and supply neutral current, $i_{sn.}$ (e) Compensated supply currents i_{sabc} and neutral current i_{sn}.

Fig. 5(c), as a result of the injected SAPF neutral current i_{cn}, shown in Fig. 5(b). However, the load neutral current i_{Ln} exists as illustrated in Fig. 5(a). A similar simulation was carried out for the system under investigation but with the conventional PI controller for the DC-link voltage control loop instead of the proposed fuzzy logic controller. The simulation results are presented in Fig. 5 parts (d)-(e) for the SAPF neutral current i_{cn} and the grid current i_{sn}, respectively. Under the proposed predictive fuzzy algorithm, the grid neutral current i_{sn} does not exceed the peak value, 14A, which was attained before the SAPF started operation. On the other hand, the classical PI control algorithm was unable to limit the transient overshoot in the grid neutral current which reaches 20A at the SAPF start-up. Both techniques attain similar steady-state results in terms of grid neutral current mitigation.

V. Experimental Verification

A laboratory prototype for the system under investigation, as shown in Fig. 6, is implemented to experimentally validate the effectiveness of the proposed compensation technique.

The proposed predictive fuzzy logic algorithm is implemented on a 32-bit, floating point, Digital Signal Processor (DSP) TMS320F28335. The SAPF is coupled to the PCC via a 4 mH interfacing inductor.

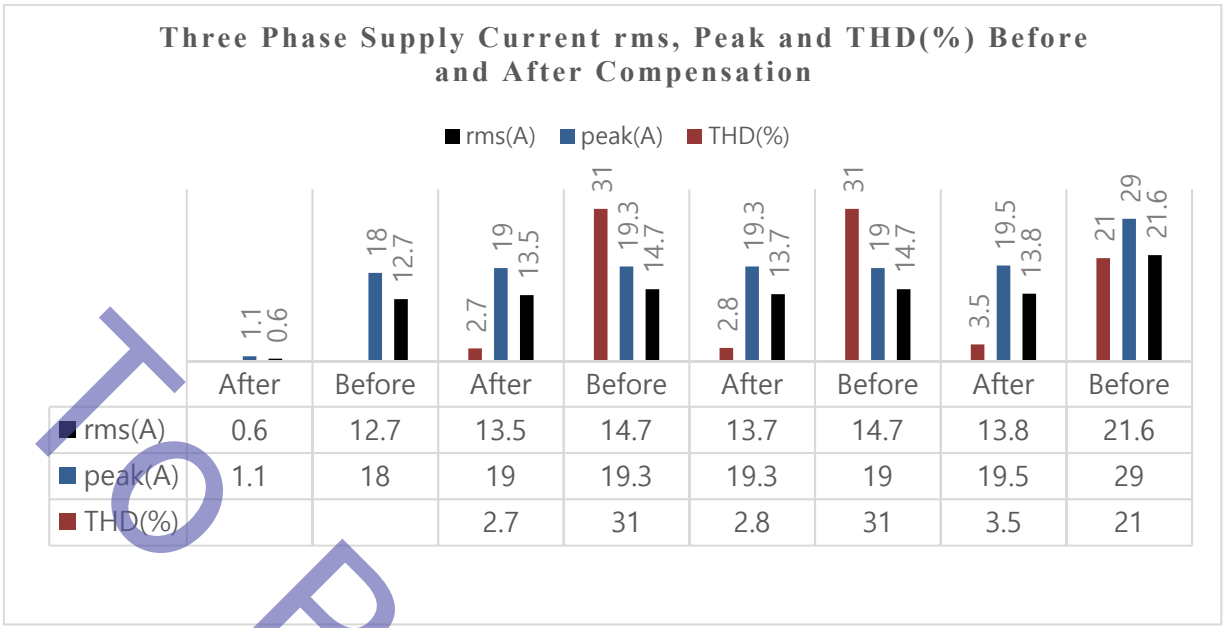

(a)

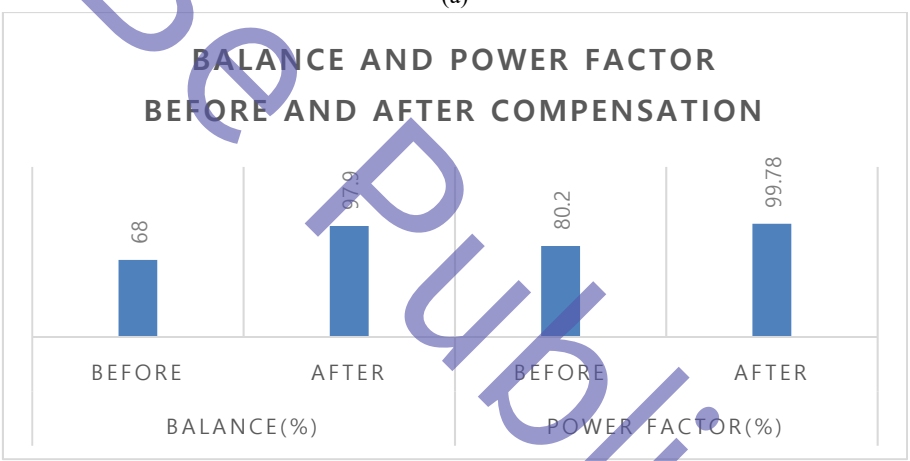

(b)

Fig. 8: Proposed controller performance analysis: (a) comparison between supply line currents rms, peak value and THD (%) before and after compensation; (b) comparison between the system balance and power factor before and after compensation.

The DC-link capacitor is 3 mF, and the SAPF inverter operates at a switching frequency of 5 kHz. The employed current and voltage sensors are LA 100-P and LV 25-P, respectively.

The practical distorted unbalanced load current, i_L, is shown in Fig. 7(a). The load current THD reaches 31% with a power factor of 0.8 and a 68% unbalance between the supply three phase currents.

The DC-link voltage is stabilized at its reference of 650V under the proposed fuzzy logic control where an overshoot of nearly 37.5% exist if the conventional PI is utilized as a DC-link voltage controller, as illustrated in Fig. 7(b). It is shown that the proposed fuzzy-logic control features a better settling time and reduced over-shoot than the classical PI control. The SAPF compensating currents are shown in Fig. 7(c). The SAPF is controlled to inject unbalanced compensating currents i_{cabc} to cancel grid current harmonics, which mitigates the supply neutral current and improves the power factor. Fig. 7(d) shows the load neutral current, i_{Ln}, the SAPF neutral compensating current, i_{cn}, and the supply neutral current, i_{sn} under the proposed predictive fuzzy-logic hybrid controller. It can be seen that the SAPF succeeded in mitigating the fourth wire supply current i_{sn}.

The compensated supply currents i_{sabc} are shown in Fig. 7(e). The THD is improved from (21%, 31% and 31%) to (3.5%, 2.8 and 2.7) for phases A, B and C, respectively, which complies with the IEEE std. 519 [6-7]. In addition, the supply power factor is improved from 0.8 to 0.997. Furthermore, the compensated supply neutral current, i_{sn}, is mitigated form (12.7A rms 18A peak) to (0.6A rms 1.1A peak). The supply rms currents i_{sabc} are reduced from (21.6A, 14.7A and 14.7A) to (13.8A, 13.7A and 13.5A) for phases A, B and C, respectively. As a result, the supply current balance is improved from 68% to 97.9%.

Moreover, the supply peak currents are reduced form (29A, 19A and 19.3A) to (19.5A, 19.3A and 19A) for phases A, B and C, respectively. The proposed predictive fuzzy hybrid control technique performance indicators are summarized in Fig. 8.

VI. Conclusions

A hybrid predictive fuzzy-logic based 4 leg SAPF control technique has been presented for low voltage distribution networks supplying unbalanced non-linear loads. The proposed technique offers enhanced performance since it succeeds in mitigating the supply current harmonics, achieves near power factor operation, offers a balanced supply current, and mitigates the neutral wire current.

Several advantages are characterized for the proposed technique since a PLL is not required, and only the supply current, supply voltage and DC-link voltage need to be measured. The presented technique effectiveness has been verified using rigorous simulations and experimental validation. In addition, the following table summarizes a comparison between the proposed technique and various recent references.

Appendix

A. MFs' Selection Using MATLAB® Fuzzy Logic Toolbox

A group of training data, based on system simulations under conventional controllers, was utilized to find the optimal MFs in the case under investigation. It is necessary to compare this result with the real one e.g. MAPE (Mean Average Percentage Error) to find less % err to find best MFs. This procedure is based on a constrained interpolations scheme, which was developed for fitting a membership function to a finite number of known membership values.

The fuzzy inference system implemented in this

TABLE II

Assessment Comparison of the Proposed Technique with Recent References

Ref. No.	***Topology***	***Harmonic current extraction method***	***Current control***	***DC-link voltage control***	***Advantages shared with the proposed technique***	***Disadvantages when compared to the proposed technique***
45	Split-Capacitor	p-q	Sliding Mode Control (SMC)	PI Controller	• PLL less	➢ Sensing the load and the filter currents are mandatory which increases system cost. ➢ Computational burden associated with the use of p-q method. ➢ Larger capacitor size is required. ➢ Higher DC-link voltage.
46	Split-Capacitor	Synchronous Reference Frame (SRF) and p-q	Dynamic Hysteresis Control	DC-link Voltage Regulator	• Low THD	➢ Sensing the load and the filter currents are mandatory which increases system cost. ➢ Computational burden associated with the use of SRF (Park and Park inverse) and two low pass filters (LPFs) of same order and cut-off frequency. ➢ Uses PLL is unavoidable.
47	Split-Capacitor	p-q	Digital Repetitive Control	Digital Repetitive Control	• PLL less • Reduced number of sensors, only measurements of supply voltage and supply current are required	➢ Sampling frequency in current control loop must be equal to the switching frequency. ➢ Eliminates only odd harmonics. ➢ DC-link voltage suffers from high oscillation and variation between the two capacitors when unbalance load is introduced. ➢ The supply voltage must be sinusoidal or the need for PLL arises.
48	Split-Capacitor	Synchronous Reference Frame (SRF)	Linear Hysteresis Control	Linear Control		➢ Sensing the load and the filter currents are mandatory which increases system cost. ➢ Need of PLL. ➢ High reference DC-link voltage of 1200 V with grid supply voltage only 220 V. ➢ Use of two large capacitors of 10 mF each.
49	Split-Capacitor	Power-Balance Theory	Power-Balance Theory	Power-Balance Theory	• PLL less	➢ Sensing the load and the filter currents are mandatory which increases system cost. ➢ Need of low-pass filter (LPF) and band-pass filter (BPF).
50	Four-Leg	Synchronous Reference Frame (SRF)	Adaptive Linear Element (Adaline)	Low Pass Filter (LPF)		➢ More number of sensors which increases system cost. ➢ Sensing the load and the filter currents is required. ➢ Computational burden associated with the use of SRF, Adaline, and LPF.

						➢ PLL is mandatory. ➢ Extremely large capacitor of 100 mF
51	Four-Leg	Non-Iterative Method	Hysteresis Control	PI Controller	• PLL less	➢ Sensing the load and the filter currents are mandatory which increases system cost
52	Split-Capacitor	Modified d–q	Hysteresis Control	PI Controller	• PLL less	➢ Sensing the load and the filter currents are mandatory which increases system cost ➢ Need of low-pass filter (LPF) and band-pass filter ➢ Higher DC-link voltage
53	Four-Leg	Synchronous Reference Frame (SRF)	Predictive Digital Current Control	Fuzzy Logic Controller		➢ Sensing the load current is mandatory which increases system cost ➢ Computational burden associated with the use of SRF (Park and Park inverse) ➢ PLL is mandatory.
Ref. No.	***Topology***	***Harmonic current extraction method***	***Current control***	***DC-link voltage control***	***Advantages shared with the proposed technique***	***Disadvantages when compared to the proposed technique***
54	Four-Leg	Synchronous Reference Frame (SRF)	Modified Resonant PI Controller	PI Controller		➢ Sensing the load and filter currents are mandatory which increases the system cost. ➢ Computational burden associated with the use of the SRF (Park and Park inverse). ➢ PLL is mandatory. ➢ Higher DC-link voltage.
55	One capacitor three-phase three-wire only	Does not need a harmonics extraction algorithm	Vector Resonant Controller	PI Controller	• Does not need a harmonics extraction algorithm	➢ This technique does not deal with system unbalance since it is only concerned with three-phase three wire. ➢ Neutral current mitigation is not considered. ➢ More sensors are required since it senses the filter current in addition to the supply current and voltage. ➢ Only blocks selected harmonics components from the load side. ➢ Requires a PLL. ➢ Uses larger size capacitors 6.6 mF.
56	One capacitor three-phase three-wire only	LPF	Source Current Detection	PI Controller		➢ This technique does not deal with system unbalance since it is only concerned with three-phase three wire. ➢ Neutral current mitigation is not considered. ➢ More sensors are required since it senses the filter current in addition to the supply current and voltage. ➢ Requires a PLL.
57	One capacitor three-phase three-wire only	Stationary Reference Frame and Synchronous Reference Frame (SRF)	SVM	PI Controller		➢ This technique does not deal with system unbalance since it is only concerned with three-phase three wire. ➢ Neutral current mitigation is not considered. ➢ More sensors are required since it senses the filter current in addition to the supply current and voltage.
58	Two capacitors three-phase three-wire only	FFT	Predictive		•PLL less •Sensing only the grid current or load current	➢ This technique does not deal with system unbalance since it is only concerned with three-phase three wire. ➢ Neutral current mitigation is not considered.
59	3-leg and H-bridge	Fundamental		PI Controller	•PLL less •Sensing only the	➢ This technique does not deal with system unbalance since it is only concerned with three-phase three wire.

	three-phase three-wire only	Extraction			grid current or load current	➢ Neutral current mitigation is not considered.
60	One capacitor three-phase three-wire only	Stationary Reference Frame and Synchronous Reference Frame (SRF)	PI-VPI Controller	PI Controller	• Reduced number of sensors, only measurements of the supply voltage and supply current are required	➢ This technique does not deal with system unbalance since it is only concerned with three-phase three wire. ➢ Neutral current mitigation is not considered. ➢ Requires a PLL.
61	Split-Capacitor	Stationary Reference Frame		Nonstandard SM – PI	• Reduced number of sensors, only measurements of the supply voltage and supply current are required	➢ Requires a PLL.
62	Split-Capacitor	Synchronous Reference Frame (SRF)	Fuzzy-Logic Current Controller	PI Controller		➢ More sensors are required since it senses the filter current in addition to the supply current and voltage. ➢ Uses a linear fuzzy controller when dealing with non-liner conditions. ➢ Requires a PLL.
63	One capacitor three-phase three-wire only	Synchronous Reference Frame (SRF)	Hysteresis Band	PI Controller and Fuzzy-logic		➢ This technique does not deal with system unbalance since it is only concerned with three-phase three wire. ➢ Neutral current mitigation is not considered. ➢Uses a linear fuzzy controller when dealing with non-liner conditions. ➢ Requires a PLL.

manuscript uses custom functions in the Fuzzy Logic Designer, available in the MATLAB Fuzzy Toolbox.

1. Open the Fuzzy Logic Designer. At the MATLAB® command line, type: fuzzyLogicDesigner.
2. Specify the number of inputs and outputs of the fuzzy system, as described in the Fuzzy Logic Designer.
3. Create custom membership functions, and replace the built-in membership functions with them, as described in Specifying Custom Membership Functions. The membership functions define how each point in the input space is mapped to a membership value between 0 and 1.
4. Create rules using the Rule Editor, as described in the Rule Editor. Define the logical relationship between the inputs and the outputs.
5. Create custom inference functions, and replace the built-in inference functions with them, as described in Specifying Custom Inference Functions. Inference methods include the AND, OR, implication, aggregation, and defuzzification methods. This action generates output values for the fuzzy system.
6. Select View > Surface to view the output of the fuzzy inference system in the Surface Viewer, as described in the Surface Viewer.

B. Part Numbers and References of The Experimental Test Rig Elements:

Hardwar	*Part number*	*Ref.*
32-bit, floating point, Digital Signal	TMS320F28335	[64]
VSI IGBTs inverter	FGH40T120SMD	[65]
Three-phase diode bridge	SGBPC50005-SGBPC5016	[66]
Voltage transducer	LV-25P	[67]
Current transducer	LA 100P	[68]

REFERENCES

[1] B. Singh, A. Chandra, and K. Al-Haddad, *Power Quality: Problems and Mitigation Techniques*: Wiley, 2015.

[2] J. Fei, *Advanced Design and Control of Active Power Filters*: Nova Science Publishers, Incorporated, 2013.

[3] A. Emadi, A. Nasiri, and S. B. Bekiarov, *Uninterruptible Power Supplies and Active Filters*: CRC Press, 2004.

[4] V. Khadkikar, A. Chandra, and B. Singh, "Digital signal processor implementation and performance evaluation of split capacitor, four-leg and three H-bridge-based three-phase four-wire shunt active filters," *IET Power Electron.*, Vol. 4, No. 4, pp. 463-470, Apr. 2011.

[5] X. Wang, F. Zhuo, J. Li, L. Wang, and S. Ni, "Modeling and control of dual-stage high-power multifunctional PV

system in d - Q - 0 coordinate," *IEEE Trans. Ind. Electron.,* Vol. 60, No. 4, pp. 1556-1570, Apr. 2013.

[6] W. R. N. Santos, E. d. M. Fernandes, E. R. C. d. Silva, C. B. Jacobina, A. C. Oliveira, and P. M. Santos, "Transformerless single-phase universal active filter with UPS features and reduced number of electronic power switches," *IEEE Trans. Power Electron.,* Vol. 31, No. 6, pp. 4111-4120, Jun. 2016.

[7] A. Salimbeni, M. Boi, I. Marongiu, M. Porru, and A. Damiano, "Integration of active filter and energy storage system for power quality improvement in microgrids," in *2016 International Symposium on Power Electronics, Electrical Drives, Automation and Motion (SPEEDAM)*, pp. 709-714, 2016.

[8] S. Prommeuan, V. Kinnares, and C. Charumit, "Control of a multifunctional 3-phase 4-wire grid connected converter using adaptive hysteresis current controller," in *Electrical Machines and Systems (ICEMS), 2014 17th International Conference on*, pp. 3234-3239, 2014.

[9] A. M. Fahmy, A. K. Abdelsalam, and A. B. Kotb, "Unified fuzzy-logic based controller for dual function 4-leg shunt APF with predictive current control," in *Power Electronics and Applications (EPE'15 ECCE-Europe), 2015 17th European Conference on*, pp. 1-10, 2015.

[10] S. A. O. d. Silva, A. F. Neto, S. G. S. Cervantes, A. Goedtel, and C. F. Nascimento, "Synchronous reference frame based controllers applied to shunt active power filters in three-phase four-wire systems," in *Industrial Technology (ICIT), 2010 IEEE International Conference on*, pp. 832-837, 2010.

[11] V. Soares, P. Verdelho, and G. D. Marques, "An instantaneous active and reactive current component method for active filters," *IEEE Trans. Power Electron.,* Vol. 15, No. 4, pp. 660-669, Jul. 2000.

[12] R. R. Sawant and M. C. Chandorkar, "A multifunctional four-leg grid-connected compensator," *IEEE Trans. Ind. Appl.,* Vol. 45, No. 1, pp. 249-259, Jan. 2009.

[13] M. Popescu, A. Bitoleanu, and V. Suru, "A DSP-based implementation of the p-q theory in active power filtering under nonideal voltage conditions," *IEEE Trans. Ind. Informat.,* Vol. 9, No. 2, pp. 880-889, May 2013.

[14] V. Khadkikar, A. Chandra, and B. N. Singh, "Generalised single-phase p-q theory for active power filtering: simulation and DSP-based experimental investigation," *IET Power Electron.,* Vol. 2, No. 1, pp. 67-78, Jan. 2009.

[15] M. Aredes, H. Akagi, E. H. Watanabe, E. V. Salgado, and L. F. Encarna, "Comparisons between the p-q and p-q-r theories in three-phase four-wire systems," *IEEE Trans. Power Electron.,* Vol. 24, No. 4, pp. 924-933, Apr. 2009.

[16] L. Chen and Z. Jia, "Three-phase four-wire shunt active power filter based on DSP," in *2010 5th IEEE Conference on Industrial Electronics and Applications*, pp. 948-951, 2010.

[17] I. I. Abdalla, K. S. R. Rao, and N. Perumal, "Three-phase four-leg shunt active power filter to compensate harmonics and reactive power," in *Computers & Informatics (ISCI), 2011 IEEE Symposium on*, pp. 495-500, 2011.

[18] S. Biricik and H. Komurcugil, "Three-level hysteresis current control strategy for three-phase four-switch shunt active filters," *IET Power Electron.,* Vol. 9, No. 8, pp. 1732-1740, Jun. 2016.

[19] V. D. Bacon and S. A. O. d. Silva, "Selective harmonic currents suppressing applied to a three-phase shunt active power filter based on adaptive filters," in *2015 IEEE 13th Brazilian Power Electronics Conference and 1st Southern Power Electronics Conference (COBEP/SPEC)*, pp. 1-6, 2015.

[20] H. Karimi, M. Karimi-Ghartemani, M. R. Iravani, and A. R. Bakhshai, "An adaptive filter for synchronous extraction of harmonics and distortions," *IEEE Trans. Power Del.,* Vol. 18, No. 4, pp. 1350-1356, Oct. 2003.

[21] N. D. Dinh, N. D. Tuyen, G. Fujita, and T. Funabashi, "Adaptive notch filter solution under unbalanced and/or distorted point of common coupling voltage for three-phase four-wire shunt active power filter with sinusoidal utility current strategy," *IET Gener., Transm. & Distrib.,* Vol. 9, No. 13, pp. 1580-1596, Oct. 2015.

[22] S. K. Chauhan, M. C. Shah, R. R. Tiwari, and P. N. Tekwani, "Analysis, design and digital implementation of a shunt active power filter with different schemes of reference current generation," *IET Power Electron.,* Vol. 7, No. 3, pp. 627-639, Mar. 2014.

[23] S. Hirve, K. Chatterjee, B. G. Fernandes, M. Imayavaramban, and S. Dwari, "PLL-less active power filter based on one-cycle control for compensating unbalanced loads in three-phase four-wire system," *IEEE Trans. Power Del.,* Vol. 22, No. 4, pp. 2457-2465, Oct. 2007.

[24] K. M. Smedley and S. Cuk, "One-cycle control of switching converters," *IEEE Trans. Power Electron.,* Vol. 10, No. 6, pp. 625-633, November 1995.

[25] S. S. E, K. P. E, K. Chatterjee, and S. Bandyopadhyay, "An active harmonic filter based on one-cycle control," *IEEE Trans. Ind. Electron.,* Vol. 61, No. 8, pp. 3799-3809, Aug. 2014.

[26] I. Purnama, P. C. Chi, Y. C. Hsieh, J. Y. Lin, and H. J. Chiu, "One cycle controlled grid-tied differential boost inverter," *IET Power Electron.,* Vol. 9, No. 11, pp. 2216-2222, Sep. 2016.

[27] Q. Chongming, J. Taotao, and K. M. Smedley, "One-cycle control of three-phase active power filter with vector operation," *IEEE Trans. Ind. Electron.,* Vol. 51, No. 2, pp. 455-463, Apr. 2004.

[28] A. Elmitwally, S. Abdelkader, and M. El-Kateb, "Neural network controlled three-phase four-wire shunt active power filter," *IEE Proc. – Gener., Transm. & Distrib.,* Vol. 147, No. 2, pp. 87-92, Mar. 2000.

[29] M. Qasim and V. Khadkikar, "Application of artificial neural networks for shunt active power filter control," *IEEE Trans. Ind. Inform.,* Vol. 10, No. 3, pp. 1765-1774, Aug. 2014.

[30] V. G. Kinhal, P. Agarwal, and H. O. Gupta, "Performance investigation of neural-network-based unified power-quality conditioner," *IEEE Trans. Power Del.,* Vol. 26, No. 1, pp. 431-437, Jan. 2011.

[31] A. Bhattacharya and C. Chakraborty, "A shunt active power filter with enhanced performance using ANN-based predictive and adaptive controllers," *IEEE Trans. Ind. Electron.,* Vol. 58, No. 2, pp. 421-428, Feb. 2011.

[32] K. Antoniewicz, M. Jasinski, M. P. Kazmierkowski, and M. Malinowski, "Model predictive control for three-level four-leg flying capacitor converter operating as shunt active power filter," *IEEE Trans. Ind. Electron.,* Vol. 63, No. 8, pp. 5255-5262, Aug. 2016.

[33] P. Acuna, L. Moran, M. Rivera, J. Dixon, and J. Rodriguez, "Improved active power filter performance for renewable power generation systems," *IEEE Trans. Power Electron.,* Vol. 29, No. 2, pp. 687-694, Feb. 2014.

[34] R. Panigrahi, B. Subudhi, and P. C. Panda, "Model predictive-based shunt active power filter with a new

reference current estimation strategy," *IET Power Electron.,* Vol. 8, No. 2, pp. 221-233, Feb. 2015.

[35] M. Odavic, V. Biagini, P. Zanchetta, M. Sumner, and M. Degano, "One-sample-period-ahead predictive current control for high-performance active shunt power filters," *IET Power Electron.,* Vol. 4, No. 4, pp. 414-423, Apr. 2011.

[36] M. S. Hamad, M. I. Masoud, B. W. Williams, and S. Finney, "Medium voltage 12-pulse converter: ac side compensation using a shunt active power filter in a novel front end transformer configuration," *IET Power Electron.,* Vol. 5, No. 8, pp. 1315-1323, Sep. 2012.

[37] M. A. A. M. Zainuri, M. A. M. Radzi, A. C. Soh, N. Mariun, and N. A. Rahim, "DC-link capacitor voltage control for single-phase shunt active power filter with step size error cancellation in self-charging algorithm," *IET Power Electron.,* Vol. 9, No. 2, pp. 323-335, Feb. 2016.

[38] R. L. d. A. Ribeiro, T. d. O. A. Rocha, R. M. d. Sousa, E. C. d. Santos, and A. M. N. Lima, "A robust DC-link voltage control strategy to enhance the performance of shunt active power filters without harmonic detection schemes," *IEEE Trans. Ind. Electron.,* Vol. 62, No. 2, pp. 803-813, Feb. 2015.

[39] S. Zhenhua, C. Chong, and H. Yanwei, "Inverse control of three-phase four-leg active power filter," in *Computer Science and Information Technology (ICCSIT), 2010 3rd IEEE International Conference on*, pp. 302-307, 2010.

[40] M. Badoni, A. Singh, and B. Singh, "Adaptive recursive inverse-based control algorithm for shunt active power filter," *IET Power Electron.,* Vol. 9, No. 5, pp. 1053-1064, Apr. 2016.

[41] A. Chebabhi, M. K. Fellah, A. Kessal, and M. F. Benkhoris, "Fuzzy logic and selectivity controllers for the paralleling of four-leg shunt active power filters based on three dimensional space vector modulation," in *Control, Engineering & Information Technology (CEIT), 2015 3rd International Conference on*, pp. 1-7, 2015.

[42] E. J. Acordi, I. N. d. Silva, and R. Q. Machado, "Application of fuzzy systems in the control of a shunt active power filter with four-leg topology," in *2014 International Joint Conference on Neural Networks (IJCNN)*, pp. 1239-1244, 2014.

[43] A. M. Fahmy, A. K. Abdelsalam, and A. B. Kotb, "4-leg shunt active power filter with hybrid predictive fuzzy-logic controller," in *2014 IEEE 23rd International Symposium on Industrial Electronics (ISIE)*, pp. 2132-2137, 2014.

[44] S. K. Jain, P. Agrawal, and H. O. Gupta, "Fuzzy logic controlled shunt active power filter for power quality improvement," *IEE Proc. - Electric Power Appl.,* Vol. 149, No. 5, pp. 317-328, Sep. 2002.

[45] V. S. Bandal, and P. N. Madurwar, "Performance analysis of shunt active power filter using sliding mode control strategies," *12th International Workshop on Variable Structure Systems (VSS)*, pp. 214-219, 2012.

[46] M. Suresh, S. S. Patnaik, Y. Suresh, and A. K. Panda, "Comparison of two compensation control strategies for shunt active power filter in three-phase four-wire system," *IEEE PES Innovative Smart Grid Technologies (ISGT)*, pp.1-6, 2011.

[47] R. Grino, R. Cardoner, R. Costa-Castello, and E. Fossas, "Digital repetitive control of a three-phase four-wire shunt active filter," *IEEE Trans. Ind. Electron.*, Vol. 54, No. 3, pp. 1495-1503, Jun. 2007.

[48] H. Y. Kanaan, S. Georges, A. Hayek, and K. Al-Haddad, "Modelling and comparative evaluation of control techniques applied to a PWM three-phase four-wire shunt active power filter," *1st IEEE Conference on Industrial Electronics and Applications*, pp. 1-6, 2006.

[49] B. N. Singh, P. Rastgoufard, B. Singh, A. Chandra, and K. Al-Haddad, "Design, simulation and implementation of three-pole/four-pole topologies for active filters," *IEE Proc. - Electric Power Appl.*, Vol. 151, No. 4, pp. 467- 476, Jul. 2004

[50] W. Lu, C. Xu, and C. Li, "Selective compensation of power quality problems with a three-phase four-leg shunt active filter," *9th World Congress on Intelligent Control and Automation (WCICA)*, pp. 166-171, 2011.

[51] P. Kanjiya, V. Khadkikar, and H. H. Zeineldin, "Optimal control of shunt active power filter to meet IEEE Std. 519 current harmonic constraints under nonideal supply condition," in *IEEE Trans. Ind. Electron.*, Vol. 62, No. 2, pp. 724-734, Feb. 2015.

[52] P. Dey and S. Mekhilef, "Current harmonics compensation with three-phase four-wire shunt hybrid active power filter based on modified D–Q theory," *IET Power Electron.*, Vol. 8, No. 11, pp. 2265-2280, Nov. 2015

[53] A. P. Sharma, J. B. Thakur, S. V. Surve, D. R. Singh and S. P. Sawant, "Comparison of PI and Fuzzy logic controller implemented in an APF for renewable Power generation," *International Conference on Energy Efficient Technologies for Sustainability (ICEETS)*, pp. 521-526, 2016.

[54] B. Kaka and A. Maji, "Performance evaluation of shunt active power filter (SAPF) connected to three phase four wire distribution networks," *IEEE International Telecommunications Energy Conference (INTELEC)*, pp. 1-9, 2016.

[55] H. Yi, F. Zhuo, Y. Zhang, Yu Li, Wenda Zhan, Wenjie Chen, and J. Liu, "A source-current-detected shunt active power filter control scheme based on vector resonant controller," *IEEE Trans. Ind. Appl.*, Vol. 50, No. 3, pp. 1953-1965, May/Jun. 2014.

[56] H. Yi, F. Zhuo, X. Wang, and J. Liu, "Study of closed-loop control scheme for source current detection type Active Power Filter," *2010 IEEE Energy Conversion Congress and Exposition*, pp. 145-150, 2010.

[57] P. Mattavelli, "A closed-loop selective harmonic compensation for active filters," *IEEE Trans. Ind. Appl.*, Vol. 37, No. 1, pp. 81-89, Jan./Feb. 2001.

[58] S. Mariethoz and A. C. Rufer, "Open loop and closed loop spectral frequency active filtering," *IEEE Trans. Power Electron.*, Vol. 17, No. 4, pp. 564-573, Jul. 2002.

[59] Z. Chen, Y. Luo, and M. Chen, "Control and performance of a cascaded shunt active power filter for aircraft electric power system," *IEEE Trans. Ind. Electron.*, Vol. 59, No. 9, pp. 3614-3623, Sep. 2012.

[60] Q. N. Trinh and H. H. Lee, "An advanced current control strategy for three-phase shunt active power filters," *IEEE Trans. Ind. Electron.*, Vol. 60, No. 12, pp. 5400-5410, Dec. 2013.

[61] R. L. d. A. Ribeiro, T. d. O. A. Rocha, R. M. de Sousa, E. C. dos Santos and A. M. N. Lima, "A robust DC-link voltage control strategy to enhance the performance of shunt active power filters without harmonic detection schemes," *IEEE Trans. Ind. Electron.*, Vol. 62, No. 2, pp. 803-813, Feb. 2015

[62] A. Elmitwally, S. Abdelkader, and M. Elkateb, "Performance evaluation of fuzzy controlled three and four wire shunt active power conditioners," *2000 IEEE Power Engineering Society Winter Meeting. Conference Proceedings (Cat. No.00CH37077)*, Vol. 3, pp. 1650-1655, 2000.

[63] K. Steela and B. S. Rajpurohit, "Enhancing performance of APF by fuzzy controller," *2014 IEEE 6th India International Conference on Power Electronics (IICPE)*, Kurukshetra, 2014, pp. 1-6.
[64] Datasheet for 32-bit, floating point, Digital Signal Processor (DSP)TMS320F28335
Online: http://www.ti.com/lit/ds/symlink/tms320f28335.pdf
[65] Datasheet for IGBTs for the inverter FGH40T120SMD Online:https://www.fairchildsemi.com/datasheets/FG/FGH40T120SMD.pdf
[66] Datasheet for Three-phase bridge SGBPC50005-SGBPC 5016, Online: http://pdf.tixer.ru/959937.pdf
[67] Datasheet for voltage trnseducer LV-25P, Online: http://www.lem.com/docs/products/lv_25-p.pdf
[68] Datasheet for caurrent trnseducer LA-100P, Online: http://www.lem.com/docs/products/la_100-p_e_.pdf

A. M. Fahmy was born in Alexandria, Egypt, on October 25, 1986. He received his B.S. degree from the Faculty of Engineering, Al-Azhar University, Cairo, Egypt, in 2009; his M.S. degree from the Arab Academy for Science and Technology (AAST), Alexandria, Egypt, in 2012; and his Ph.D. degree in Electrical Engineering from Al-Azhar University, Cairo, Egypt, in 2016. From 2010 to 2015, he was a Teaching Assistant at the AAST. On May 2016, he joined the Canadian International College (CIC), Cairo, Egypt, as Lecturer. His current research interests include power quality and distributed generation. Dr. Fahmy is a Member of the IEEE Power Electronics Society.

Ahmed K. Abdelslam was born in Alexandria, Egypt, on March 4, 1980. He received his B.S. and M.S. degrees from the Faculty of Engineering, Alexandria University, Alexandria, Egypt, in 2002 and 2006, respectively; and his Ph.D. degree in Electrical Engineering from the College of Engineering, University of Strathclyde, Glasgow, SCT, UK, in 2009. From 2010 to 2011, was a Postdoctoral Research Associate in the Department of Electrical and Computer Engineering, Texas A&M University at Qatar (TAMUQ), Al Rayyan, Qatar. In March 2011, he started working as an Assistant Professor at the Arab Academy for Science and Technology (AAST), Alexandria, Egypt. On May 2015, he was promoted to Associate Professor at AAST. His current research interests include motor drives, power quality, distributed generation, and power converters for renewable energy systems. He is a Co-Founder of the Renewable Energy and Power Electronic Application (REPEA) Research Center. Dr. Abdelsalam is a Member of the IEEE Power Electronics Society, the IEEE Industrial Electronics Society, and the Institute of Engineering and Technology (IET).

Ahmed A. Lotfy received his B.S., M.S. and Ph.D. degrees from Alexandria University, Alexandria, Egypt, in 1982, 1989 and 1997, respectively. He worked with Schindler Lifts, Alexandria, Egypt, in several sectors as Field Engineer, in the technical office and finally as a Senior Engineer and as Manager of the Maintenance and Repair Department. In 1994, he joined the Arab Maritime Transport Academy (AMTA), Alexandria, Egypt (currently the Arab Academy for Science, Technology and Maritime Transport (AASTMT)). Since 2008, he has been working as a Professor in the Department of Electrical and Control Engineering, College of Engineering and Technology. From 2010 to 2012, Dr. Lotfy was a Vice-Dean for Postgraduate Studies and Research, College of Engineering and Technology. He is presently the Dean of Faculty Affairs at AASTMT. His current research interests include HVDC, FACTS, renewable energy, power system protection, high voltage engineering and reliability. Dr. Lotfy is a Senior Member of the IEEE. He is also a Member of the IEEE Dielectrics and Electrical Insulation Society, the IEEE Power and Energy Society, the IEEE Reliability Society, and the IEEE Technology and Engineering Management Society.

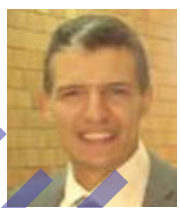

Mostafa Hamad received his B.S. and M.S. degrees in Electrical Engineering from Alexandria University, Alexandria, Egypt, in 1999 and 2003, respectively; and his Ph.D. degree in Electrical Engineering from the University of Strathclyde, Glasgow, SCT, UK, in 2009. From 2010 to 2014, he was an Assistant Professor in the Department of Electrical and Control Engineering, College of Engineering and Technology, Arab Academy for Science, Technology and Maritime Transport (AASTMT), Alexandria, Egypt, where he is presently working as an Associate Professor. His current research interests include power electronics applications, power quality, electric drives, distributed generation, HVDC transmission systems, and renewable energy.

Abdesamee Kotb received his B.S., M.S. and Ph.D. degrees in Electrical Engineering from Al-Azhar University, Cairo, Egypt, in 1973, 1976 and 1982, respectively. Since 1993, he has been working as a Professor at Al-Azhar University. His current research interests include electric drives, electrical machines, and power quality.